Oxidative addition of iodine, iodomethane and iodobenzene to the rhodium phosphino enolate complex $[\overline{\mathrm{Rh}\{\mathrm{Ph_2PCH}\overset{\cdots}{-}\mathrm{C}(\overset{\cdots}{-}\mathrm{O}}\mathrm{)Ph\}(CO)(PPh_3)}]$ and carbon monoxide insertion into the resulting Rh–carbon bond of $[\overline{\mathrm{Rh}\{\mathrm{Ph_2PCH}\overset{\cdots}{-}\mathrm{C}(\overset{\cdots}{-}\mathrm{O}}\mathrm{)Ph\}Me(I)(CO)(PPh_3)}]$

Pierre Braunstein,*[a] Yves Chauvin,[b] Jean Fischer,[c] Hélène Olivier,*[b] Carsten Strohmann[d] and Dawn V. Toronto[b]

[a] *Laboratoire de Chimie de Coordination (CNRS UMR 7513), Université Louis Pasteur, 4 rue Blaise Pascal, F-67070 Strasbourg cedex, France. E-mail: braunst@chimie.u-strasbg.fr*
[b] *Institut Français du Pétrole, BP 311, F-92506 Rueil-Malmaison, France*
[c] *Laboratoire de Cristallochimie et de Chimie Structurale (CNRS UMR 7513), Université Louis Pasteur, 4 rue Blaise Pascal, F-67070 Strasbourg cedex, France*
[d] *Institut für Anorganische Chemie, Universität Würzburg, Am Hubland, D-97074 Würzburg, Germany*

Received (in Montpellier, France) 2nd February 2000, Accepted 27th March 2000

The oxidative addition of homo- and heteronuclear molecules XI (X = I, Me, Ph) to the square planar rhodium phosphino enolate complex $[\overline{\mathrm{Rh}\{\mathrm{Ph_2PCH}\overset{\cdots}{-}\mathrm{C}(\overset{\cdots}{-}\mathrm{O}}\mathrm{)Ph\}(CO)(PPh_3)}]$ **1** afforded the hexacoordinate Rh(III) complexes $[\overline{\mathrm{Rh}\{\mathrm{Ph_2PCH}\overset{\cdots}{-}\mathrm{C}(\overset{\cdots}{-}\mathrm{O}}\mathrm{)Ph\}X(I)(CO)(PPh_3)}]$ (X = Me **2**; X = Ph **3**; X = I **4**). Complex **2** undergoes CO insertion into the Rh–Me bond to afford three isomers of the acetyl species $[\overline{\mathrm{Rh}\{\mathrm{Ph_2PCH}\overset{\cdots}{-}\mathrm{C}(\overset{\cdots}{-}\mathrm{O}}\mathrm{)Ph\}\{C(O)Me\}(I)(CO)(PPh_3)}]$ **5a**–**c**. Two of these isomers lose acetyl iodide to regenerate **1** and these transformations were followed by NMR and IR spectroscopic methods. The reaction of **1** with acetyl chloride results in rapid formation of the acetyl complex $[\overline{\mathrm{Rh}\{\mathrm{Ph_2PCH}\overset{\cdots}{-}\mathrm{C}(\overset{\cdots}{-}\mathrm{O}}\mathrm{)Ph\}\{C(O)Me\}(Cl)(CO)(PPh_3)}]$ **6**. When left in solution, **6** isomerizes to give two additional isomeric acetyl species. All three isomers rapidly decompose to a Rh(I) species. The crystal structures of **1–3** have been determined by X-ray diffraction. The coordination geometry around the rhodium atom of **2** and **3** is distorted octahedral and the alkyl and halide ligands are in a mutually *trans* position.

Introduction

β-Ketophosphines such as $\mathrm{Ph_2PCH_2C(O)Ph}$ and keto (or imino) phosphorus ylides such as $\mathrm{Ph_3P{=}CHC(O)Ph}$ represent key ligands for the formation of phosphino enolate metal complexes, a class of compounds of growing importance. Such complexes may be obtained by deprotonation of the α-methylene group of (coordinated) β-ketophosphines[1] or by oxidative addition of a P–aryl bond of phosphorus ylides across a transition metal complex, respectively, although only Ni(0) complexes have been reported to perform this reaction.[2] Phosphino enolate complexes have been described for many transition metals, such as Re, Fe, Ru, Co, Rh, Ni, Pd and Pt.[1,3] They contain one or more planar chelate rings and are generally very stable, although they display interesting reactivity patterns. Provided that such complexes contain a metal–carbon or metal–hydrogen bond (or that such bonds could be formed in an activation step), a catalytic species may be obtained whose reactivity can be tuned by the steric and electronic properties of the substituents on the phosphino enolate chelating ligand. Thus, nickel phosphino enolate complexes are known to catalyze the oligomerization of ethylene into α-olefins[2,4] (Shell Higher Olefin Process), the polymerization of ethylene to high molecular weight polyethylene[5] and the co-oligomerization with polar monomers.[6] Catalyst activity, average chain length and degree of branching of the polymer are strongly dependent on the phosphino enolate ligand. Furthermore, ylide-substituted Ni phosphino enolates are highly active catalysts for acetylene polymerization.[7]

Recent work in our laboratories has produced a variety of phosphino enolate derivatives of Ni(II), Pd(II), Rh(I), Rh(III), Ru(II) and Ir(I);[8,9] some of them led to active homogeneous catalysts. For example, Rh(I) complexes such as $[\overline{\mathrm{Rh}\{\mathrm{Ph_2PCH}\overset{\cdots}{-}\mathrm{C}(\overset{\cdots}{-}\mathrm{O}}\mathrm{)Ph\}(CO)(PPh_3)}]$ **1** have proved to be active in catalytic hydrogenation of alkenes and in transfer dehydrogenation of alkanes to alkenes.[9] These results led us to develop the chemistry of phosphino enolate Rh(I) complexes more extensively. Since oxidative addition reactions across a transition metal centre represent key processes in many catalytic reactions, such as carbonylation, hydrogenation or oligomerization, our aim was to investigate the activity of phosphino enolate complexes in such reactions. We first studied the addition of iodine derivatives and then the activity of the Rh(III) complexes thus obtained as regards insertion reactions. The oxidative addition of various organic halides to Rh(I) carbonyl phosphine complexes has been extensively studied, particularly in the case of iodomethane, largely because of its relevance to the catalytic carbonylation of methanol.[10–15] The effect of monoanionic bidendate ligands containing donor atoms, such as O, N, or S, in five- or six-membered chelate rings on the formation of isomeric forms of methyl, carbonyl or acetyl Rh(III) complexes has been widely discussed.[16–20] Chelating ligands of the phosphino enolate type (*P*,*O*) are expected to induce more selectivity in

DOI: 10.1039/b000961j

the coordination sphere of a metal than chelates with identical donor atoms. Here, we focus on the reactivity of **1**[9] towards the oxidative addition of iodine derivatives and the possible insertion of carbon monoxide into the newly formed metal–carbon bond.

Results and discussion

Synthesis of complexes resulting from oxidative addition

Complex **1**, whose crystal structure is described below, reacted with an excess of MeI, PhI, or one equivalent of I_2 to give Rh(III) complexes, as shown in eqn. (1). In all these products, the ligands X and I are *trans* with respect to each other.

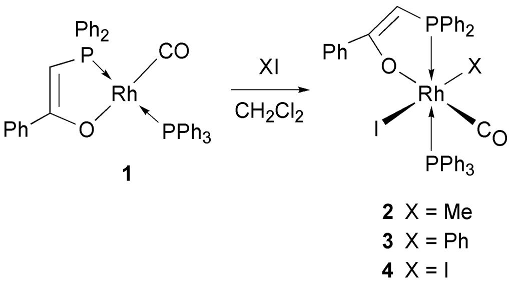

(1)

The addition of a 10-fold excess of iodomethane to a dichloromethane solution of **1** resulted in a colour change from pale orange to yellow. Concentration of the solution and addition of diethyl ether afforded yellow crystals of $[\mathrm{Rh}\{\mathrm{Ph_2PCH{\cdots}C({\cdots}O)Ph}\}\mathrm{Me(I)(CO)(PPh_3)}]$ **2**, whose structure has been determined crystallographically (*vide infra*). The PhI analogue was synthesized by dissolving **1** in neat iodobenzene and heating under light reflux. The formation of $[\mathrm{Rh}\{\mathrm{Ph_2PCH{\cdots}C({\cdots}O)Ph}\}\mathrm{Ph(I)(CO)(PPh_3)}]$ **3** was accompanied by a darkening of the yellow solution. Concentration of the solution led to the formation of yellow crystals of **3**, which were analyzed by X-ray diffraction to unambiguously determine the molecular stereochemistry (*vide infra*). IR monitoring of the formation of **2** and **3** showed the reaction to be complete when the ν(CO) absorption at 1969 $\mathrm{cm^{-1}}$ was replaced by a new band at 2046 or 2051 $\mathrm{cm^{-1}}$, respectively.

Addition of one equivalent of I_2 to a dichloromethane solution of **1** made the yellow solution turn red and IR spectroscopy [ν(CO), 2080 $\mathrm{cm^{-1}}$] showed the immediate formation of a Rh(III) oxidative addition product. Addition of diethyl ether produced a red powder that has been characterized as $[\mathrm{Rh}\{\mathrm{Ph_2PCH{\cdots}C({\cdots}O)Ph}\}\mathrm{(I)_2(CO)(PPh_3)}]$ **4**, based on its similar spectroscopic properties, compared to **2** and **3**. The ligand arrangement was confirmed by X-ray diffraction, although the quality of the structure is too poor for publication.[21]

The $\nu(\mathrm{C{\cdots}O}) + \nu(\mathrm{C{\cdots}C})$ absorption of the phosphino enolate ligand in the Rh(III) complexes **2**–**4** appears to be unaffected by the change in electron density at the rhodium centre and remains at 1525 $\mathrm{cm^{-1}}$, as found in the precursor complex **1**. This has also been observed for the Rh(I) square planar complexes $[\mathrm{Rh}\{\mathrm{Ph_2PCH{\cdots}C({\cdots}O)Ph}\}\mathrm{(CO)(L)}]$ [L = $\mathrm{PMe_3}$, $\mathrm{P(}o\mathrm{\text{-}tolyl)_3}$, $\mathrm{PPh_2(}p\mathrm{\text{-}tolyl)}$, $\mathrm{P(}p\mathrm{\text{-}FC_6H_4)_3}$],[9] where the enolate system delocalizes the electron density at the metal centre, which results in a carbonyl stretching frequency almost independent of the Brönsted basicity of the phosphine ligand (at least in the range explored). When the oxidation state of the metal is increased, the donor properties of the phosphino enolate ligand do not compensate for the decrease in electron density and this is reflected in an increase of the stretching frequency of the carbonyl group. The trend in ν(CO) absorption, I > Ph > Me, agrees with the higher oxidative character of iodine compared to phenyl iodide and methyl iodide and reflects the slightly π acidic nature of the phenyl group. This has also been observed with complexes of the form $[\mathrm{Rh(quinaldinate)(CO)(PR_3)}]$ and in their oxidative addition products.[19]

The $^{31}\mathrm{P}\{^1\mathrm{H}\}$ NMR spectra of complexes **2**–**4** show an ABX (A, B = P, X = Rh) pattern with a strong ^2J(P,P) coupling diagnostic of a *trans* arrangement of the phosphorus atoms. In the parent complex **1**, a doublet for the enolate phosphorus atom and a broad singlet for the triphenylphosphine ligand were observed, indicating that, at room temperature, dissociation of triphenylphosphine occurred.[9] The presence of dissociated triphenylphosphine always resulted in the formation of a small quantity (<5%) of $[\mathrm{MePPh_3}]^+\mathrm{I}^-$ during the synthesis of **2**. Increasing the MeI : **1** molar ratio above 100 : 1 lowered the yield of **2** and increased the percentage of phosphonium salt produced.

The ^{1}H NMR spectra of $\mathrm{CD_2Cl_2}$ solutions of **2** and **3** contain characteristic resonances, confirming the addition of the methyl and phenyl group, respectively. For **2**, the methyl protons give rise to a triplet of doublets at δ 0.78 as a result of coupling to rhodium and the *cis*-phosphorus atoms. For all three complexes, the signal corresponding to the enolate proton appears as a doublet of doublets around δ 5.30. These NMR data are consistent with the presence of only one isomer in solution. Spectroscopic details for complexes **2**–**4** are given in the Experimental section.

Reaction of complex 2 with carbon monoxide

The reaction was monitored by $^{31}\mathrm{P}\{^1\mathrm{H}\}$ NMR spectroscopy. When 0.2 MPa of carbon monoxide was applied to a $\mathrm{CD_2Cl_2}$ solution of **2** at room temperature for 1 h, its characteristic doublet of doublets resonance at δ 14.5 and 46.1 with ^1J(Rh,P) = 92 and 89 Hz and ^2J(P,P) = 412 Hz was depleted while new ABX patterns (A = B = P, X = Rh) appeared, which were assigned to the acetyl complex $[\mathrm{Rh}\{\mathrm{Ph_2PCH{\cdots}C({\cdots}O)Ph}\}\{\mathrm{C(O)Me}\}\mathrm{(I)(CO)(PPh_3)}]$ **5** (3 stereoisomers **5a**–**c**) and **1** (Scheme 1). The magnitude of ^2J(P, P) (between 340 and 410 Hz) suggests that the phosphorus atoms retain the *trans* arrangement present in **2**. The acetyl, carbonyl and iodo ligands therefore occupy positions *cis* to both the phosphino enolate phosphorus atom and the triphenylphosphine ligand. For such an arrangement, there are six possible isomeric structures representing three pairs of enantiomers and this is consistent with the spectroscopic data. The IR spectrum exhibits a characteristic band at 1679 $\mathrm{cm^{-1}}$ for an acetyl ligand on Rh(III) that is very strong and slightly asymmetric and may thus contain the absorptions corresponding to each isomer.

Based on similar carbonylation studies and the kinetic preference for the *cis* isomer over the *trans* isomer,[22,23] the first set of resonances seen in the $^{31}\mathrm{P}\{^1\mathrm{H}\}$ NMR spectrum is assigned to one of the two structures with a mutual *cis* arrangement of the acetyl and iodide ligands (**5a** δ_A 8.5, δ_B 41.0; Scheme 1), but the exact stereochemistry is uncertain. The other sets were assigned to **5b** (δ_A 5.4, δ_B 45.4) and **5c** (δ_A – 1.8, δ_B 40.2). Unfortunately, IR and ^{13}C NMR studies (*vide infra*) did not provide spectroscopic data allowing us to distinguish between the stereoisomers. As the reaction continues, the resonances for **5a** and **5b** reach a maximum intensity and then begin to diminish, those for **5c** reach a maximum and remain constant and the resonances due to **1** continue to grow. Eventually, the two species remaining in solution are **5c** and **1**, implying that reductive elimination of acetyl iodide has occurred from **5a** and/or **5b**. It is well established that a concerted reductive elimination process can only occur between *cis* ligands and that the *trans* configuration is thermodynamically more stable; therefore, the remaining set of ABX resonances in the NMR spectrum is assigned to the *trans* isomer **5c**. The mechanism of the elimination reaction of acetyl iodide has been well established in the catalytic carbonylation of

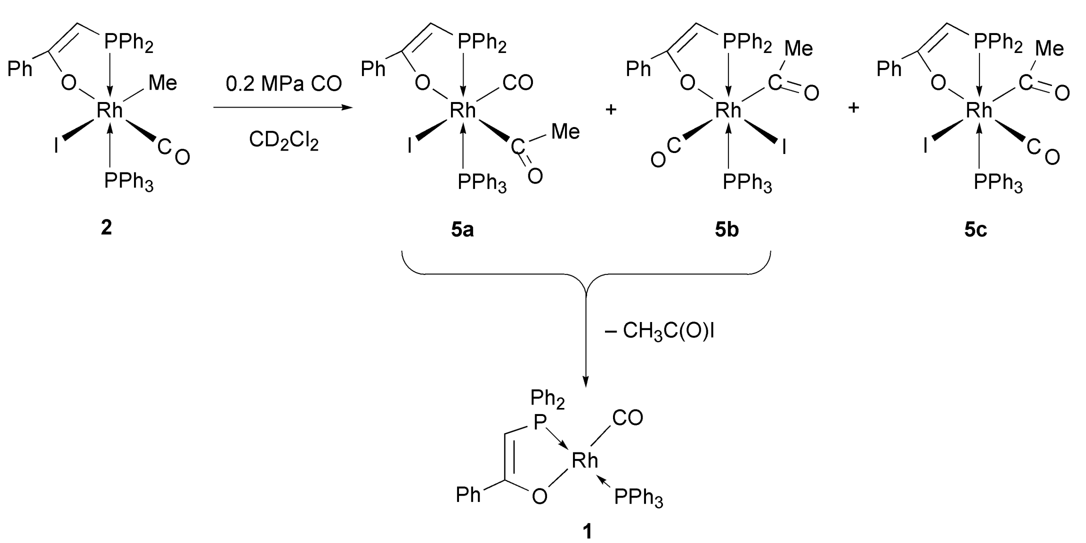

Scheme 1

methanol by rhodium complexes.[24] Scheme 1 depicts a similar route, with the formation of complex **1** arising from the elimination of acetyl iodide from either of the *cis* intermediates **5a** or **5b**.

Isomerization of **5a** could also account for the formation of **5b** and **5c**. Separate studies show that, while **5a** isomerizes in solution, the rate of this process is too slow to contribute significantly to the formation of **5b** and **5c**. A CD_2Cl_2 solution of **2** was reacted with 0.2 MPa of carbon monoxide for a period of 1–4 h after which time the reaction was quenched. The best results were found after a reaction period of 4 h under CO, although the kinetic isomer **5a** was never formed exclusively without **5b** and **5c**. Shorter reaction times did not allow a sufficient build-up of **5a**. After 4 h under CO, **5a** accounts for approximately 1/3 of the organometallic products visible. The remaining constituents **2**, **5c**, **5b**, and **1** are present in the ratio 8 : 2 : 1 : 2. Quenching the reaction by release of CO pressure did not result in decarbonylation of the acyl species **5a**–**c** and monitoring by both ^{1}H NMR and ^{31}P{^{1}H} NMR spectroscopies showed that after three days there is very little change in the resonance intensities for either the acetyl proton peaks or the phosphorus peaks. While interconversion does occur amongst the three isomers, the rate is too slow to contribute significantly to the formation of these isomers during the carbonylation reaction. It is interesting that the more reactive ruthenium complex $[\text{Ru(Me)(I)(CO)}_2(\text{PMe}_3)_2]$ readily adds carbon monoxide at −30 °C to give *cis*-$[\text{Ru}\{\text{C(O)Me}\}(\text{I})(\text{CO})_2(\text{PMe}_3)_2]$, which rapidly converts to the *trans* isomer at 10 °C.[25] Under similar conditions, **2** was found to be unreactive towards carbon monoxide.

Under reaction conditions similar to those used for **2**, complex **3** was found to be unreactive towards carbon monoxide insertion. This appears to be due to a relatively strong Rh–phenyl bond,[25] which favours the phenyl over the benzoyl complex. Kinetic and mechanistic studies of the acyl(benzoyl)-alkyl(aryl) rearrangement of *para*-substituted benzoyl rhodium complexes have shown that this rearrangement is irreversible and proceeds in only one direction to yield the aryl complex,[26a] whereas the reaction of the methyl complex proceeds only in the opposite direction and favours formation of the acetylrhodium complex. Similarly, in the reactions $[\text{RhR(CO)(PPh}_3)_2\text{Cl}_2] \rightleftharpoons [\text{Rh}\{\text{C(O)R}\}(\text{PPh}_3)_2\text{Cl}_2]$ the acyl form is favoured for R = Me while the equilibrium is strongly shifted to the left when R = Ph.[26b–d] Note, however, that faster migration of phenyl over methyl in a direct transformation, $\text{RhR(CO)} + \text{L} \rightarrow \text{Rh}\{\text{C(O)R}\}\text{L}$, has been observed in other rhodium complexes.[26e,f]

The stereochemical pathway to carbonylation can occur either through methyl migration to a *cis*-carbon monoxide ligand or through formal CO insertion into a *cis*-methyl–rhodium bond.[27,28] Although our studies do not distinguish between the two pathways, methyl migration has been shown to predominate in a variety of carbonylation studies and is the most common mechanism of the alkyl–acyl rearrangement observed with organometallic complexes,[29] including a variety of $[\text{Rh(Y)Me(I)(CO)(PR}_3)_2]$ and $[\text{RhMe(I)(CO)(PPh}_3)(\text{MBL})]$ species (Y = anionic ligand, MBL = monoanionic bidentate ligand).[17,18] There are two possible routes available for methyl migration, depending mainly on the ease of substitution of one of the anionic ligands by carbon monoxide and on the solvent used.[23] Acyl formation can occur either through an ionic intermediate by reversible substitution of the anionic ligand by CO, methyl migration to the *cis*-carbonyl and recoordination of the anion (Scheme 2) or through direct methyl migration to a *cis*-carbonyl group *via* an unsaturated 5-coordinated intermediate (presumably square pyramidal for low spin rhodium d^6 complexes), which rapidly isomerizes and adds carbon monoxide (Scheme 3).[23,30]

For example, carbonylation of the ruthenium compounds $[\text{RuMe(Y)(CO)}_2(\text{PMe}_3)_2]$ (Y = I, CN),[23] in which the metal–anion bond strengths are high, proceeds *via* a mechanism similar to that in Scheme 3 rather than *via* anion substitution. For the phosphino enolate compound **2**, CO insertion is likely to occur according to Scheme 3, assuming that the soft iodide dissociates less readily from the rhodium atom, as found in ruthenium complexes. In fact, this appears to be consistent with the lower reactivity of **2** (*ca.* 4 h) with AgOTf in CH_2Cl_2 to give the triflate salt $[\text{Rh}\{\text{Ph}_2\text{PCH}{\overset{\cdot\cdot}{=}}\text{C}({\overset{\cdot\cdot}{=}}\text{O})\text{Ph}\}\text{Me(CO)(PPh}_3)](\text{OTf})$ **7**[31] when compared to the ruthenium complex $[\text{RuMe(I)(CO)}_2(\text{Pr}^i\text{-DAB})]$ (Pr^i-DAB = Pr^{i}N=CHCH=NPr^i), which reacts with AgOTf quantitatively after 15 min to form $[\text{RuMe(CO)}_2(\text{Pr}^i\text{-}$

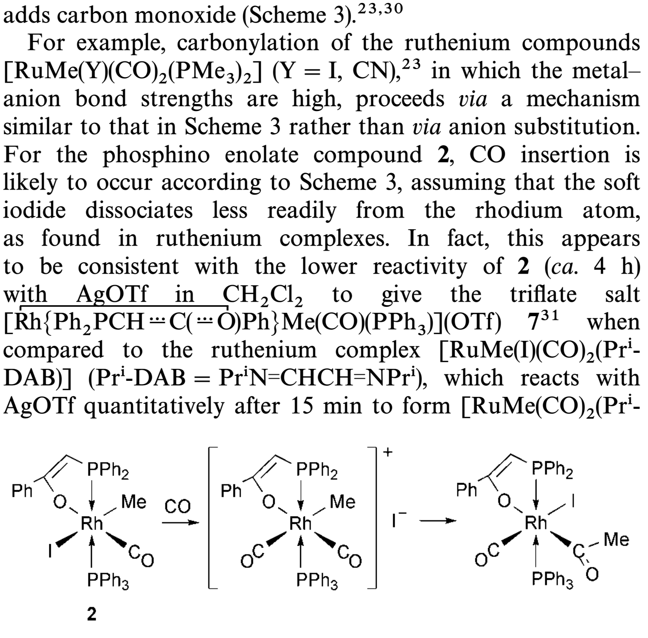

Scheme 2

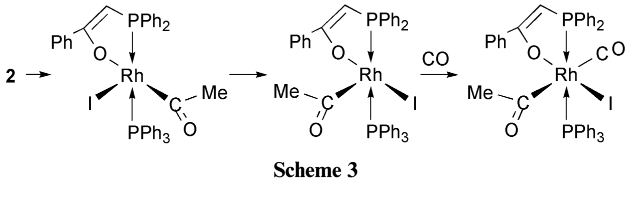

Scheme 3

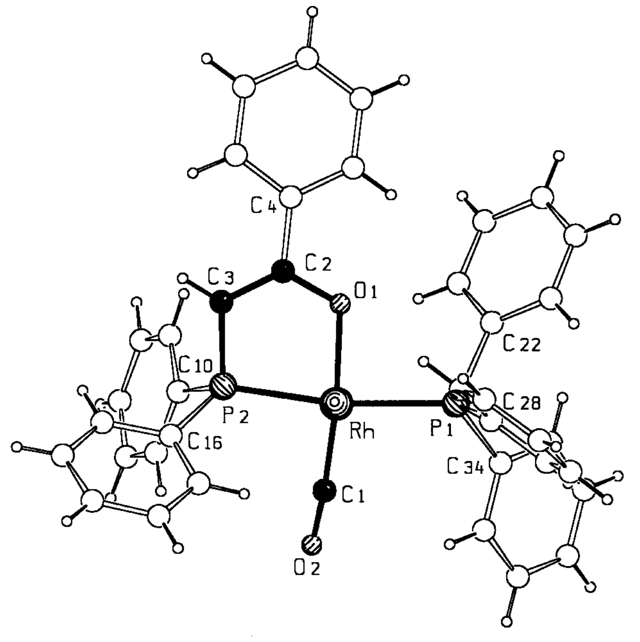

Fig. 1 View (Schakal) of the structure of $[\overline{\text{Rh}\{\text{Ph}_2\text{PCH}=\text{C}(=\text{O}})\text{Ph}\}(\text{CO})(\text{PPh}_3)]$ **1**.

DAB)](OTf).[32] Assuming that the pathway in Scheme 3 is operative in the carbonylation of **2**, methyl migration to give a 5-coordinate square pyramidal intermediate followed by isomerization and then coordination of the incoming CO group would explain the formation of the three isomers seen in the NMR spectrum. Such a behaviour finds precedent in a recent study by Baker *et al.*[22] in which spectroscopic data consistent with a 5-coordinate intermediate that adds CO to give two stereoisomers of $[\text{Rh}\{\text{C(O)Me}\}(\text{I})_2\{\text{Ph}_2\text{PCH}_2\text{P(S)Ph}_2\}(\text{CO})]$ were reported. Based on NMR data, these authors suggested a mutual *trans* arrangement of the phosphorus and iodide ligands, thus providing a system in which all three enantiomeric pairs of isomers possible would have the correct *cis* arrangement of acetyl and iodide ligands to reductively eliminate acetyl iodide. However, spectroscopic evidence for only two such isomers was obtained.

Unlike in other studies,[15d,22] a 5-coordinate intermediate and its isomerization products have not been observed by spectroscopic methods. Thus, whether isomerization occurs before or after CO insertion cannot be specified. Several studies in the past few years have emphasized the importance of the former isomerization process in establishing the identity of the mechanism of oxidative addition of iodomethane to Rh(I) complexes.[33] Isomerization from the primary oxidative addition product is always an available pathway, resulting in a different ground state structure for the thermodynamic product. While the solid state structure of **2** suggests an ionic S_N2 two-step mechanism, the final *trans* arrangement of the methyl and iodide ligands could have resulted from a concerted three-centre *cis*-addition followed by rapid isomerization. That no intermediate could be detected during the synthesis of **2** or during its carbonylation could be due to the relatively slow oxidative addition reaction of **1** with MeI and the slow rate of carbonylation of **2**.

In an attempt to follow the reaction by $^{13}\text{C}\{^1\text{H}\}$ NMR spectroscopy, labeled $^{13}\text{CH}_3\text{I}$ was used in the synthesis of **2**. The ^{13}C analogue of **2** shows coupling to rhodium and two phosphorus atoms, resulting in a doublet of triplets centered at δ 14. Mirroring both the ^1H and $^{31}\text{P}\{^1\text{H}\}$ NMR data, the $^{13}\text{C}\{^1\text{H}\}$ NMR study shows the immediate formation of a singlet at δ 20.2 assigned to the acetyl ligand of isomer **5a**. As the reaction progresses, two new singlets grow at δ 20.3 and 20.1, which correspond to the increasing formation of isomers **5b** and **5c**, respectively, while eventually only the peak at δ 20.1 remains. Identification of the acyl carbon by $^{13}\text{C}\{^1\text{H}\}$ NMR spectroscopy was unsuccessful due to insufficient intensity of the unlabeled carbonyl group signal and the distribution of its intensity over three isomers with different chemical shifts. Details of the $^{13}\text{C}\{^1\text{H}\}$ NMR data for complex **2** are reported in the Experimental section.

To complement the NMR studies, IR monitoring of the carbonylation of **2** was carried out in CD_2Cl_2 at room temperature. Upon addition of carbon monoxide, a new band grows at 1679 cm^{-1}, characteristic of an acyl complex. As the reaction progresses, this band increases in intensity and the carbonyl band of **2** at 2045 cm^{-1} broadens and shifts to higher energy as **2** is consumed and replaced by the less electron rich acyl complexes **5a–c**. The $\nu(\text{C}=\text{O}) + \nu(\text{C}=\text{C})$ enolate absorption at 1525 cm^{-1} remains unchanged. After a short induction period, an additional carbon monoxide absorption appears at 1969 cm^{-1}. This peak is characteristic of the Rh(I) complex **1**, which is formed upon reductive elimination of acetyl iodide. Throughout the course of the reaction, only one observable acyl stretch at 1679 cm^{-1} and one carbonyl stretch at 2050 cm^{-1} appear in the IR spectrum, indicating that the three isomers are indistinguishable by IR. Very similar observations have been made for the two isomers of $[\text{Rh}\{\text{C(O)Me}\}(\text{I})_2\{\text{Ph}_2\text{PCH}_2\text{P(S)Ph}_2\}(\text{CO})]$.[22] In agreement with the NMR results, the IR spectrum at the end of the reaction shows absorptions due mainly to the presence of **1**, and low intensity carbon monoxide and acyl absorptions due to the remaining isomer **5c**.

Isolation of the acyl complexes for further characterization was unsuccessful. We therefore attempted the direct synthesis of $[\overline{\text{Rh}\{\text{Ph}_2\text{PCH}=\text{C}(=\text{O}})\text{Ph}\}\{\text{C(O)Me}\}\text{Cl}(\text{CO})(\text{PPh}_3)]$ by addition of acetyl chloride to **1** [eqn. (2)]. $^{31}\text{P}\{^1\text{H}\}$ NMR monitoring of this reaction in CD_2Cl_2 at room temperature indicated the formation of a rhodium acetyl species **6a** with an ABX pattern centered at δ_A 3.7 and δ_B 45.0.

$$\underset{\mathbf{1}}{\overline{\text{Rh}\{\text{Ph}_2\text{PCH}=\text{C}(=\text{O}})\text{Ph}\}(\text{CO})(\text{PPh}_3)} + \text{MeC(O)Cl} \rightarrow \underset{\mathbf{6}}{\overline{\text{Rh}\{\text{Ph}_2\text{PCH}=\text{C}(=\text{O}})\text{Ph}\}\{\text{C(O)Me}\}\text{Cl}(\text{CO})(\text{PPh}_3)} \quad (2)$$

A new ^1H NMR resonance appeared as a singlet at δ 2.19 whereas the enolate resonance gave rise to a doublet of doublets at δ 5.42. The IR spectrum showed a carbon monoxide absorption at 2075 cm^{-1} and an absorption around 1675 cm^{-1} arising from the acetyl group. This acyl complex is not stable, and within 10 min a light yellow powder begins to precipitate and the $^{31}\text{P}\{^1\text{H}\}$ NMR resonances due to **6a** diminish while a doublet at δ 27 and two new complexes with an ABX pattern appear. As the sample ages, other unidentified phosphine-containing products are formed. Filtration and spectroscopic analysis of the yellow powder in CDCl_3 showed it to be responsible for the doublet at δ 27 [$^1J(\text{Rh,P}) = 127$ Hz]. The ^1H NMR spectrum shows only aromatic protons and the IR spectrum contains a carbon monoxide absorption at 1975 cm^{-1}, indicative of a Rh(I) complex. These data are consistent with the presence of $[\text{RhCl(CO)(PPh}_3)_2]$. Analysis of the mother liquor by IR and NMR revealed that a rhodium acyl complex remained in solution. Similar to the reactions studied by Wilkinson and coworkers on acyl halide addition to Rh(I) complexes,[26b,34] the acyl complex **6a** is unstable with respect to isomerization and decomposition, as shown in the ^{31}P NMR spectrum by the growth of the peaks at δ_A 24.4, δ_B 42.9 (**6b**) and δ_A 18.5, δ_B 45.1 (**6c**).

Solid **6a** was isolated as a slightly impure flaky solid upon immediate solvent removal at the end of the reaction. If placed in dichloromethane, a similar sequence of decomposition and isomerization occurs as was found during the synthesis. Like

6a, **6b** and **6c** are unstable and readily decompose. Bearing in mind literature reports, this instability is not surprising.[34,35] For the formation of stable rhodium complexes of this type to occur a delicate balance must exist between steric and electronic factors.[36] Without a crystal structure of either **5** or **6** it is difficult to evaluate the different steric demands of the ligands. On purely steric grounds, the larger iodide ion should lead to greater steric crowding and result in an acyl complex less stable than the chloride derivative. In fact, our results show the opposite. Note, however, that steric effects may be more complicated to analyze and conformational effects have also been found to play a considerable role on the rate of migratory CO insertion on rhodium.[15d] The greater stability of **5a**–**c** over **6a**–**c** suggests the participation of electronic effects.

Crystal structures

[Rh{Ph$_2$PCH$\doteq$C($\doteq$O)Ph}(CO)(PPh$_3$)] 1. This complex crystallizes with half a molecule of diethyl ether per formula unit. Selected interatomic distances and angles are given in Table 1. The molecular structure is shown in Fig. 1. The square planar environment of the rhodium atom is similar to that in [Rh{Ph$_2$PCH$_2$C(O)Ph}(CO)(PPh$_3$)]PF$_6$, which, in contrast to **1**, contains a neutral ketophosphine ligand.[9] As expected, the Rh–O(1) bond is shorter in **1** [2.059(2) Å] than in [Rh{Ph$_2$PCH$_2$C(O)Ph}(CO)(PPh$_3$)]PF$_6$ [2.084(4) Å], whereas in both complexes the carbon–oxygen distances in the CO ligand are similar [1.151(4) and 1.144(9) Å, respectively]. In both complexes, the Rh–P distance involving the chelating ligand is shorter than that to the PPh$_3$ ligand, 2.2793(9) *vs.* 2.3588(8) Å in **1** and 2.281(3) *vs.* 2.343(3) Å in [Rh{Ph$_2$PCH$_2$C(O)Ph}(CO)(PPh$_3$)]PF$_6$. The C–H bond of the enolato moiety is localized in the P(2)–C(3)–C(2) plane. The P(2)–C(3) distance of 1.761(3) Å is slightly longer than the corresponding P–CH$_2$ distance in [Rh{Ph$_2$PCH$_2$C(O)Ph}(CO)(PPh$_3$)]PF$_6$, consistent with the sp^2 character of the carbon atom in the former case. When compared with the CH$_2$–C(Ph) and C=O distances in [Rh{Ph$_2$PCH$_2$C(O)Ph}(CO)(PPh$_3$)]PF$_6$, the C(2)–C(3) and C(2)–O(1) distances in **1** are, respectively, shorter [1.363(4) *vs.* 1.505(9) Å] and longer [1.320(4) *vs.* 1.252(6) Å], which is consistent with the electronic delocalization within the enolate moiety and a strong double bond character for the C(2)–C(3) bond.

[Rh{Ph$_2$PCH$\doteq$C($\doteq$O)Ph}Me(I)(CO)(PPh$_3$)] 2. This complex crystallizes with one molecule in the asymmetric unit. Selected interatomic distances and angles are given in Table 2. The molecular structure is shown in Fig. 2. The coordination polyhedron corresponds to a distorted octahedral geometry in which there is a mutual *trans* relationship between the oxygen atom of the bidentate enolate ligand and the carbon atom of the CO ligand, the methyl and the iodide ligands, the triphenylphosphine ligand and the phosphorus atom of the enolate. The largest distortions from octahedral geometry are seen in the following angles: O(1)–Rh–C(21) 83.2(2)°, P(1)–Rh–O(1) 82.5(1)° and I–Rh–C(22) 101.0(2)°. The non-bonded distance between C(22)$\cdots$C(21), 2.80 Å, when compared to the computed van der Waals distance, 3.6 Å, indicates a strong repulsive interaction between the methyl and carbon monoxide ligand. Other neighbouring contacts are also repulsive in nature: O(1)$\cdots$I 3.33 Å (vdW = 3.55 Å), O(1)$\cdots$C(21) 2.78 Å (vdW = 3.40 Å), I$\cdots$C(22) 3.61 Å (vdW = 3.75 Å), with the latter interaction being the least repulsive due to the widening of the I–Rh–C(22) angle by 11°. The rhodium–ligand bond distances observed in **2** are compared in Table 3 to those of the related Rh(III) complexes *trans*-[RhMe(I)(ox)(CO)(PPh$_3$)],[37] where ox is 8-hydroxyquinoline, and *cis*-[RhMe(I)(quin)(CO){P(4-MeC$_6$H$_4$)$_3$}],[19] where quin is 2-quinaldinate

Table 1 Selected bond lengths (Å) and angles (deg) for [Rh{Ph$_2$PCH$\doteq$C($\doteq$O)Ph}(CO)(PPh$_3$)] **1**

Rh–C(1)	1.803(3)	P(2)–C(3)	1.761(3)
Rh–O(1)	2.059(2)	P(2)–C(10)	1.823(3)
Rh–P(2)	2.2793(9)	P(2)–C(16)	1.825(3)
Rh–P(1)	2.3588(8)	O(1)–C(2)	1.320(4)
P(1)–C(28)	1.824(3)	O(2)–C(1)	1.151(4)
P(1)–C(22)	1.826(3)	C(2)–C(3)	1.363(4)
P(1)–C(34)	1.834(3)	C(2)–C(4)	1.491(4)
C(1)–Rh–O(1)	174.16(11)	C(10)–P(2)–C(16)	103.67(14)
C(1)–Rh–P(2)	91.61(10)	C(3)–P(2)–Rh	100.61(11)
O(1)–Rh–P(2)	82.54(6)	C(2)–O(1)–Rh	118.7(2)
C(1)–Rh–P(1)	97.46(10)	O(2)–C(1)–Rh	175.1(3)
O(1)–Rh–P(1)	88.38(6)	O(1)–C(2)–C(3)	122.9(3)
P(2)–Rh–P(1)	170.92(3)	0(1)–C(2)–C(4)	114.4(2)
C(3)–P(2)–C(10)	106.8(2)	C(3)–C(2)–C(4)	122.5(3)
C(3)–P(2)–C(16)	109.1(2)	C(2)–C(3)–P(2)	114.7(2)

Table 2 Selected bond lengths (Å) and angles (deg) for [Rh{Ph$_2$PCH$\doteq$C($\doteq$O)Ph}Me(I)(CO)(PPh$_3$)] **2**

Rh–P(1)	2.318(1)	Rh–O(1)	2.079(3)
Rh–P(2)	2.418(1)	C(22)–O(2)	1.123(6)
Rh–C(21)	2.104(6)	C(1)–O(1)	1.314(6)
Rh–I	2.7854(5)	C(1)–C(2)	1.368(7)
Rh–C(22)	1.824(5)	P(1)–C(2)	1.741(5)
I–Rh–C(21)	168.1(2)	P(1)–Rh–C(21)	86.8(2)
I–Rh–C(22)	101.0(2)	P(1)–Rh–C(22)	93.7(2)
I–Rh–O(1)	85.0(1)	P(2)–Rh–I	89.51(3)
O(1)–Rh–C(21)	83.2(2)	P(2)–Rh–O(1)	94.1(1)
O(1)–Rh–C(22)	173.0(2)	P(2)–Rh–C(21)	93.0(2)
C(21)–Rh–C(22)	90.7(2)	P(2)–Rh–C(22)	89.8(2)
P(1)–Rh–P(2)	176.53(5)	Rh–C(22)–O(2)	176.0(2)
P(1)–Rh–O(1)	82.5(1)	P(1)–C(2)–C(1)	116.5(4)
P(1)–Rh–I	89.98(4)	C(2)–C(1)–O(1)	123.3(4)
		C(1)–O(1)–Rh	118.0(2)

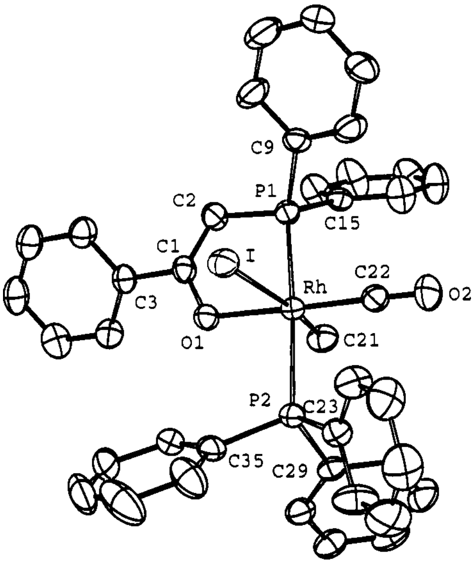

Fig. 2 View (ORTEP) of the structure of [Rh{Ph$_2$PCH$\doteq$C($\doteq$O)Ph}Me(I)(CO)(PPh$_3$)] **2**. Thermal ellipsoids are drawn at the 30% probability level.

Table 3 Comparison of bond lengths (Å) between **2**, *cis*-[RhMe(I)(quin)(CO){P(4-MeC$_6$H$_4$)}] **A** and *trans*-[RhMe(I)(ox)(CO)(PPh$_3$)] **B**

	2	**A**	**B**
Rh–I	2.7854(5)	2.701(2)	2.809(1)
Rh–CH$_3$	2.104(6)	2.11(1)	2.104(8)
Rh–O	2.079(3)	2.039(9)	2.036(4)
Rh–PPh$_3$	2.418(1)	2.334(3)	2.317(2)
Rh–CO	1.824(5)	1.81(1)	1.866(7)

anion. The overall structure of **2** is typical of alkyl halide Rh(III) oxidative addition products. The Rh–C(21)H_3 bond distance in **2** [2.104(6) Å] compares well with the values observed in both the quin and ox complexes cited above. The Rh–I bond [2.7854(5) Å] is elongated with respect to the quin complex by 0.084 Å due to the strong *trans* influence of the methyl group but agrees well with the Rh–I distance found in *trans*-[RhMe(I)(ox)(CO)(PPh_3)] [2.809(1) Å].

The lengthening of the rhodium–triphenylphosphine bond in **2** distinguishes this complex from the quin and ox analogues. The Rh–PPh_3 bond distance in **2** [2.418(1) Å] is significantly longer than the Rh–PPh_3 distances in *cis*-[RhMe(I)(quin)(CO){P(4-MeC_6H_4)$_3$}] [2.334(3) Å] or *trans*-[RhMe(I)(ox)(CO)(PPh_3)] [2.317(2) Å]. This trend complies with the decreasing *trans* influence P > N > I. The Rh–P(2) distance is also 0.10 Å longer than the bond between the rhodium and the phosphorus atom of the enolate ligand; thus the *trans* influence of the two phosphorus atoms results in a lengthening of the Rh–P bond of the triphenylphosphine ligand, while the Rh–P bond of the phosphino enolate ligand is relatively unaffected.

The Rh–C(22)O and Rh–O(1) bond distances are similar to those found in the *cis* and *trans* adducts. The remaining distances and angles found in the phosphino enolate ligand and triphenylphosphine ligand are unexceptional. The C–O [1.314(6) Å] and C–C [1.368(7) Å] bond distances within the enolate ligand compare well with those in **1** and in other Rh(III) enolate complexes in which electronic delocalization leads to bond orders intermediate between single and double bonds.

$[\overline{\text{Rh}\{\text{Ph}_2\text{PCH}\overset{\cdots}{-}\text{C}(\overset{\cdots}{-}\text{O}})\text{Ph}\}\text{Ph(I)(CO)(PPh}_3)]$ 3. This complex crystallizes with one molecule in the asymmetric unit. Selected interatomic distances and angles are given in Table 4. The molecular structure is shown in Fig. 3.

The coordination geometry is similar to the corresponding iodomethane oxidative addition product. The C(21), C(27), I, O(1) array is relatively planar although significant distortion is observable in the compression of the P(2)–Rh–O(1) angle [83.61(6)°] and the accompanying widening of the P(2)–Rh–C(27) angle [99.8(1)°). As a result of the bidentate nature of the phosphino enolate ligand, the P(1)–Rh–O(1) bond angle is also compressed [83.34(6)°]. These distortions result in a 13° deviation from linearity for the P(1)–Rh–P(2) bond axis.

Overall a change from methyl to phenyl does not greatly disturb the system. Non-bonding interactions between the carbon monoxide and the alkyl or aryl ligands are observed in **2** and **3**, respectively. The distances for the $CH_3\cdots CO$ interaction (2.80 Å) and the Ph···CO interaction (2.81 Å) show that these groups fit snugly between neighbouring atoms.

Table 4 Selected bond lengths (Å) and angles (deg) for $[\overline{\text{Rh}\{\text{Ph}_2\text{PCH}\overset{\cdots}{-}\text{C}(\overset{\cdots}{-}\text{O}})\text{Ph}\}\text{Ph(I)(CO)(PPh}_3)]$ **3**

Rh–P(1)	2.3285(8)	Rh–O(1)	2.052(2)
Rh–P(2)	2.4164(8)	C(27)–O(2)	1.128(5)
Rh–C(21)	2.078(3)	C(2)–O(1)	1.308(4)
Rh–I	2.7752(3)	C(1)–C(2)	1.364(5)
Rh–C(27)	1.859(4)	P(1)–C(1)	1.749(4)
I–Rh–C(21)	175.9(1)	P(1)–Rh–C(27)	93.4(1)
I–Rh–C(27)	84.9(1)	P(1)–Rh–C(21)	89.75(9)
I–Rh–O(1)	92.67(7)	P(2)–Rh–I	93.28(2)
O(1)–Rh–C(21)	91.5(1)	P(2)–Rh–O(1)	83.61(6)
O(1)–Rh–C(27)	175.9(1)	P(2)–Rh–C(21)	87.48(9)
C(21)–Rh–C(27)	90.9(2)	P(2)–Rh–C(27)	99.8(1)
P(1)–Rh–P(2)	166.59(3)	Rh–C(27)–O(2)	176.1(1)
P(1)–Rh–O(1)	83.34(6)	P(1)–C(1)–C(2)	116.8(3)
P(1)–Rh–I	90.43(2)	C(1)–C(2)–O(1)	123.7(3)
		C(2)–O(1)–Rh	117.9(1)

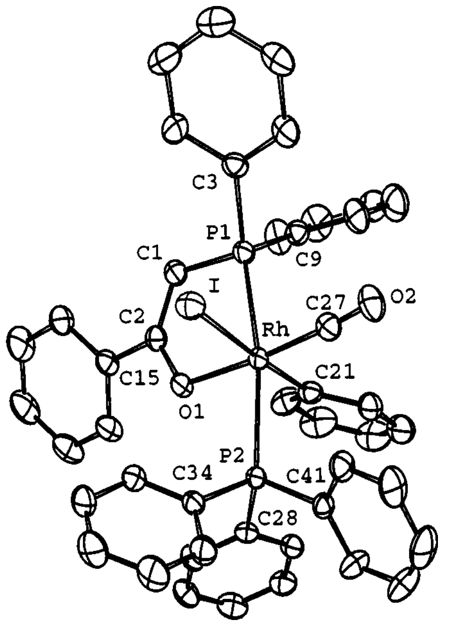

Fig. 3 View (ORTEP) of the structure of $[\overline{\text{Rh}\{\text{Ph}_2\text{PCH}\overset{\cdots}{-}\text{C}(\overset{\cdots}{-}\text{O}})\text{Ph}\}\text{Ph(I)(CO)(PPh}_3)]$ **3**. Thermal ellipsoids are drawn at the 30% probability level.

The metal–ligand bond distances in complex **3** are similar to those in complex **2**. The Rh–I bond distance [2.7752(3) Å] indicates that the phenyl, like the methyl group [Rh–I bond 2.7854(5) Å], exerts a large *trans* influence. Complexes having a ligand with a small *trans* influence opposite the Rh–I bond usually have this bond falling within the 2.60–2.69 Å range. The Rh–C(21) distance in **3** [2.078(3) Å] is shorter than the Rh–C(21)H_3 distance in **2** [2.104(6) Å] as a result of the carbon sp^2 hybridized orbital used in forming the metal–ligand bond of the former. The shorter, stronger bond is also responsible for the failure of **3** to insert carbon monoxide. The rhodium–triphenylphosphine bond in **3** [Rh–P(2) 2.4164(8) Å] is also elongated with respect to the rhodium–phosphino enolate bond [Rh–P(1) 2.3285(8) Å] and like **2**, is considerably longer than the metal–phosphine distances found for the related complexes tabulated in Table 3. The Rh–P bond in both **2** and **3** is also approximately 0.03 Å longer than the corresponding bonds in [Rh(acac)$(I)_2(PPh_3)_2$] containing the *trans*-oriented P–Rh–P unit.[38] The bond distances within the enolate ligand again indicate electronic delocalization.

Conclusions

Previous studies have shown that the oxidative addition of a covalent molecule to square planar carbonylphosphine rhodium(I) complexes containing a monoanionic bidentate ligand results in the formation of either *cis*/*trans* addition products or acyl complexes. Ligand variations have a marked effect on the Lewis basicity of the metal centre and thus play a major role in determining the reactivity, mechanism and final ground state stereochemistry of the products formed. The oxidative addition reactions to the enolate complex **1** were therefore of interest due to the different σ and π properties given by the *P,O* ligand and the effects of this new metal–ligand interaction on the nucleophilicity of the metal complex. In addition, the presence of the carbon monoxide ligand offered the interesting possibility of obtaining the 5-coordinate acetyl complex $[\overline{\text{Rh}\{\text{Ph}_2\text{PCH}\overset{\cdots}{-}\text{C}(\overset{\cdots}{-}\text{O}})\text{Ph}\}\{\text{C(O)R}\}\text{(I)(PPh}_3)]$ as the final product.

Our results show that **1** readily adds a variety of XI-type substrates to give stable oxidative addition products, resulting in all cases from a net *trans* addition of XI. For X = Me and Ph, the molecular structures were determined crystallographically and show that for both **2** and **3** the rhodium atom is placed in a distorted octahedral coordination sphere with similar bond distances and angles within the two structures. The shorter Rh–C(21) bond found in the phenyl analogue [2.078(3) Å, **3** *vs.* 2.104(6) Å, **2**] results from greater orbital overlap between the empty rhodium d_{z^2} orbital and the sp^2 hybrid orbital of the phenyl carbon. In **2** the Rh–C(21)H_3 bond is formed between the rhodium d_{z^2} orbital and the sp^3 hybrid orbital of the methyl carbon. The stronger bond of the former becomes important during the carbonylation studies where CO insertion reactions do not occur. On the other hand, if **2** is placed under 0.2 MPa carbon monoxide, insertion occurs to give three isomers of the acetyl complex $[\overline{\mathrm{Rh\{Ph_2PCH{=}C({=}O}}\mathrm{)Ph\}\{C(O)Me\}(I)(CO)(PPh_3)}]$ **5**. Although the mechanism of insertion was not determined, it likely occurs by formal methyl migration to a *cis* carbon monoxide ligand, generating a dynamic 5-coordinate square pyramidal intermediate; isomerization and coordination of carbon monoxide results in the formation of the three isomers. Formation of complex **1** by reductive elimination of acetyl iodide was observed. If one assumes a concerted process for the elimination of acetyl iodide from the *cis* isomers of **5**, a *cis* geometry of **5a** and **5b** and a *trans* geometry of **5c** result. The latter is the sole isomer left in solution at the end of the reaction.

Interestingly, the reaction between **1** and acetyl chloride also leads to the formation of three isomers, **6a–c**. These isomers share similar spectroscopic properties with **5a–c**. Isomers **6b** and **6c** are generated by isomerization of **6a**, which can be isolated in an impure state. If **6a** is left in solution, it isomerizes and decomposes to $[RhCl(CO)(PPh_3)_2]$; after formation, the isomers **6b** and **6c** also quickly decompose. The decomposition pathway remains undetermined but clearly involves loss of the enolate ligand and a redistribution of ligands.

The acetyl complexes generated by reaction of **2** with CO are significantly more stable than their chloride analogues, which were synthesized directly by oxidative addition of acetyl chloride to **1**. This difference suggests the involvement of electronic effects, rather than steric considerations.

Experimental

Reagents and physical measurements

All operations were performed in Schlenk-type flasks under high purity argon although complexes **2**–**4**, **5** and **6** appear to be air stable. Solvents were dried and distilled under argon: toluene and diethyl ether from sodium–benzophenone, dichloromethane over NaH, methanol, iodomethane, and iodobenzene from 3 Å molecular sieves. Acetyl chloride was distilled prior to use. ^1H NMR spectra were recorded on a FT Bruker AC-F 200 NMR spectrometer that operates at 200 MHz. $^{31}P\{^1H\}$ NMR were recorded on a FT Bruker CXP 200 NMR spectrometer that operates at 81 MHz. Carbonylation studies were made using a high pressure NMR tube, which contained *ca.* 148 mmol of complex **2** in 0.5 mL CD_2Cl_2. The sample was degassed on the line three times by freeze–pump thawing and then 0.25 MPa carbon monoxide was added. Both ^1H and $^{31}P\{^1H\}$ NMR spectra of the carbonylation reaction of **2** were taken every 1 to 4 h up to completion of the reaction (*ca.* 60 h). Chemical shifts (in ppm) are referenced to deuterated solvent for ^1H and $^{13}C\{^1H\}$ NMR spectra and to external 85% phosphoric acid standard for $^{31}P\{^1H\}$ NMR spectra using the highfield positive convention for reporting chemical shifts. IR spectra were recorded in the 4000–200 cm^{-1} region on a Perkin Elmer 883 IR spectrometer. Samples were prepared as Nujol mulls or in CD_2Cl_2 solution using CaF_2 cells. IR spectra of the carbonylation reaction of **2** were taken using two different methods.

Method 1: A CD_2Cl_2 solution of **2** (143 mmol) was introduced into a 0.106 mm KBr cell and a CO pressure of 0.16 MPa was applied. Spectra were taken approximately every hour on a digilab FTS80 IR spectrometer. Method 2: A sample was prepared as described in the NMR section and at various time intervals the reaction was arrested by releasing the CO pressure. This solution was then placed into a CaF_2 IR cell and the spectrum was recorded. Both methods gave identical results, however the reaction proceeded more rapidly with method 2 due to the greater CO pressure that is accessible with the NMR tube and the greater surface area of mixing between the gas and the liquid in the NMR tube.

Synthesis

Published methods were used to prepare **1**.[9]

$[\overline{\mathrm{Rh\{Ph_2PCH{=}C({=}O}}\mathrm{)Ph\}Me(I)(CO)(PPh_3)}]$ **2.** To 250 mg (0.358 mmol) of complex **1** dissolved in 5 mL of dichloromethane was added 224 μL (3.60 mmol) of MeI. After 1 h of stirring, the light orange solution turned yellow; the volume was reduced to 2 mL and diethyl ether added to precipitate the yellow crystalline powder: 265 mg (89%); This compound can be recrystallized from dichloromethane–diethyl ether. IR (CH_2Cl_2): $\nu(CO)$ 2046(vs), $\nu(C{=}O) + \nu(C{=}C)$ 1525(s) cm^{-1}. ^1H NMR (CD_2Cl_2): δ 0.78 (m, 3H, CH_3),5.29 [dd, $^2J(P,H) = 5.4$, $^3J(Rh,H) = 2.2$ Hz, 1H, PCH], 7.2–8.0 (m, 30H, Ph). $^{13}C\{^1H\}$ NMR (CD_2Cl_2): δ 14.2 [dt, $^1J(Rh,C) = 21$, $^2J(P,C) = 3$ Hz, CH_3], 70.1 [dd, $^1J(P,C) = 67$, $^2J(Rh,C) = 1$ Hz, PCH], 184.0 [d, $^1J(Rh,C) = 16$, $^2J(P,C) = 7$ Hz, PhCO], 187.2 [dt, $^1J(Rh,C) = 60$, $^2J(P,C) = 11$ Hz, CO]. $^{31}P\{^1H\}$ NMR (CD_2Cl_2): δ_A 14.5 [dd, PPh_3, $^1J(Rh,P) = 92$ Hz], δ_B 46.1 [dd, PCH, $^1J(Rh,P) = 89$, $^2J(P_A,P_B) = 412$ Hz].

$[\overline{\mathrm{Rh\{Ph_2PCH{=}C({=}O}}\mathrm{)Ph\}Ph(I)(CO)(PPh_3)}]$ **3.** To 226 mg (0.321 mmol) of complex **1** was added 5 mL of PhI. A gentle reflux was applied for 2 h, after which time the yellow solution darkened. The progress of this reaction was monitored by IR and was complete when the CO stretch at 1979 cm^{-1} was replaced by the new CO stretch at 2051 cm^{-1}. Excess PhI was removed by distillation to give a mixture of yellow crystals and a brown yellow gum. The mixture was dissolved in a minimum of dichloromethane and diethyl ether was added to precipitate the yellow crystalline powder: 202 mg (77%). IR (CH_2Cl_2): $\nu(CO)$ 2051(vs), $\nu(C{=}O) + \nu(C{=}C)$ 1525(s) cm^{-1}. ^1H NMR (CD_2Cl_2): δ 6.2–6.6 (m, 5H, Ph), 5.25 [dd, $^2J(P,H) = 5.4$, $^3J(Rh,H) = 3.5$ Hz, 1H, PCH], 6.8–7.9 (m, 30H, Ph). $^{31}P\{^1H\}$ NMR (CD_2Cl_2): δ_A 13.9 [dd, PPh_3, $^1J(Rh,P) = 89$ Hz], δ_B 49.4 [dd, PCH, $^1J(Rh,P) = 87$, $^2J(P_A,P_B) = 408$ Hz].

$[\overline{\mathrm{Rh\{Ph_2PCH{=}C({=}O}}\mathrm{)Ph\}(I)_2(CO)(PPh_3)}]$ **4.** To 222 mg (0.320 mmol) of complex **1** dissolved in 5 mL of dichloromethane was added 0.081 mg (0.320 mmol) of I_2. Upon addition the pale yellow solution turned red. After stirring for 30 min, the volume was reduced to 2 mL and diethyl ether was added to precipitate the dark red crystalline powder: 262 mg (86%). This compound can be recrystallized from dichloromethane–diethyl ether. IR (CH_2Cl_2): $\nu(CO)$ 2080(vs), $\nu(C{=}O) + \nu(C{=}C)$ 1525(s) cm^{-1}. ^1H NMR (CD_2Cl_2): δ 5.45 [dd, $^2J(P,H) = 6.6$, $^3J(Rh,H) = 2.4$ Hz, 1H, PCH], 6.2–7.2 (m, 30H, Ph). $^{31}P\{^1H\}$ NMR (CD_2Cl_2): δ_A 1.3 [dd, PPh_3, $^1J(Rh,P) = 79$ Hz], δ_B 34.9 [dd, PCH, $^1J(Rh,P) = 76$, $^2J(P_A,P_B) = 469$ Hz].

$[\overline{\mathrm{Rh\{Ph_2PCH{=}C({=}O}}\mathrm{)Ph\}\{C(O)Me\}Cl(CO)(PPh_3)}]$ **6a–c.** To 300 mg (0.431 mmol) of complex **1** dissolved in 7 mL of dichloromethane was added 30 μL (0.422 mmol) of MeC(O)Cl. After stirring for *ca.* 10 min, the solvent was quickly removed by vacuum techniques to give 311 mg (93%) of a yellow flaky solid. This compound cannot be recrystallized due to its instability in solution and is always contaminated with small quantities of decomposition products. IR (CH_2Cl_2): ν(CO) 2075(vs), 1675 (vs), $\nu(C\overset{\cdots}{-}O) + \nu(C\overset{\cdots}{-}C)$ 1525(s) cm^{-1}. ^1H NMR (CD_2Cl_2): **6a**, δ 2.19 [s, $C(O)CH_3$], 5.42 [dd, $^2J(P,H) = 5.4$, $^3J(Rh,H) = 2.2$ Hz, PCH], 7.2–8.0 (m, 30H, Ph). $^{31}P\{^1H\}$ NMR (CD_2Cl_2): δ_A 11.7 [dd, PPh_3, $^1J(Rh,P) = 100$ Hz], δ_B 45.0 [dd, PCH, $^1J(Rh,P) = 95$, $^2J(P_A,P_B) = 347$ Hz]. **6b**, $^{31}P\{^1H\}$ NMR (CD_2Cl_2): δ_A 24.4 [dd, PPh_3, $^1J(Rh,P) = 93$ Hz], δ_B 42.9 [dd, PCH, $^1J(Rh,P) = 91$, $^2J(P_A,P_B) = 312$ Hz]. **6c**, $^{31}P\{^1H\}$ NMR (CD_2Cl_2): δ_A 18.5 [dd, PPh_3, $^1J(Rh,P) = 100$ Hz], δ_B 45.1 [dd, PCH, $^1J(Rh,P) = 95$, $^2J(P_A,P_B) = 344$ Hz].

$[\overline{Rh\{Ph_2PCH\overset{\cdots}{-}C(\overset{\cdots}{-}O})Ph\}Me(CO)(PPh_3)](OSO_2CF_3)$ 7. To 300 mg (0.431 mmol) of complex **2** dissolved in 50 mL of dichloromethane was added 440 mg (1.71 mmol) solid $AgOSO_2CF_3$. After 5 h of stirring, the yellow solution darkened and AgI precipitated. The solution was filtered over Celite and reduced to dryness to give a flaky yellow solid. The formation of this complex was accompanied by a small amount of $[MePPh_3]I$: 185 mg (51%). IR (CH_2Cl_2): ν(CO) 2090(vs), $\nu(C\overset{\cdots}{-}O) + \nu(C\overset{\cdots}{-}C)$ 1550(s), ν(OTf) 1280(vs) cm^{-1}. ^1H NMR (CD_2Cl_2): δ 1.55 (br s, 3H, CH_3), 5.13 [d, $^2J(P,H) = 7$ Hz, 1H, PCH], 6.9–8.0 (m, 30H, Ph). $^{31}P\{^1H\}$ NMR (CD_2Cl_2): δ_A 15.6 (br s), δ_B 55.8 [d, $^1J(Rh,P_B) = 129$ Hz].

Crystal structure determinations

Crystal data for 1. $C_{39}H_{31}O_2P_2Rh \cdot 0.5Et_2O$, $M = 733.6$, monoclinic, space group $P2_1/n$, $a = 13.864(3)$, $b = 8.859(2)$, $c = 29.696(6)$ Å, $\beta = 101.27(3)°$, $U = 3577.0(13)$ Å^3, $Z = 4$, $\mu(\text{Mo-K}_\alpha) = 0.602$ mm^{-1}, $T = 293$ K. A total of 25 660 reflections with 6624 [R(int) = 0.0536] independent reflections were collected, with 5690 reflections having $F_o > 4\sigma(F_o)$. $R = 0.0365$ [$I > 2\sigma(I)$], $wR_2 = 0.1066$ (all data).[39]

Crystal data for 2. $C_{40}H_{34}O_2P_2RhI$, $M = 838.5$, monoclinic, space group $P2_1/n$, $a = 12.054(3)$, $b = 24.130(3)$, $c = 12.213(3)$ Å, $\beta = 92.25(2)°$ $U = 3549(2)$ Å^3, $Z = 4$, $\mu(\text{Mo-K}_\alpha) = 1.455$ mm^{-1}, $T = 294$ K. A total of 8297 reflections with 4491 [R(int) = 0.032] independent reflections were collected with 4991 reflections having $I > 3\sigma(I)$. $R(F) = 0.039$, $Rw(F) = 0.055$.[40]

Crystal data for 3. $C_{45}H_{36}O_2P_2RhI$, $M = 900.5$, orthorhombic, space group $Pna2_1$, $a = 17.887(5)$, $b = 18.538(5)$, $c = 11.515(5)$ Å, $U = 3818(3)$ Å^3, $Z = 4$, $\mu(\text{Mo-K}_\alpha) = 1.377$ mm^{-1}, $T = 294$ K. A total of 6390 reflections were collected with 5141 reflections having $I > 3\sigma(I)$. $R(F) = 0.022$, $Rw(F) = 0.027$.[40] The absolute structure was determined by refining Flack's x parameter.

CCDC reference number 440/178. See http://www.rsc.org/suppdata/nj/b0/b000961j/ for crystallographic files in .cif format.

Notes and references

1 (*a*) S.-E. Bouaoud, P. Braunstein, D. Grandjean, D. Matt and D. Nobel, *Inorg. Chem.*, 1986, **25**, 3765; (*b*) S.-E. Bouaoud, P. Braunstein, D. Grandjean, D. Matt and D. Nobel, *Inorg. Chem.*, 1988, **27**, 2279; (*c*) F. Balegroune, P. Braunstein, D. Grandjean, D. Matt and D. Nobel, *Inorg. Chem.*, 1988, **27**, 3320; (*d*) P. Braunstein, D. Matt, D. Nobel, F. Balegroune, S.-E. Bouaoud, D. Grandjean and J. Fischer, *J. Chem. Soc.*, *Dalton Trans.*, 1988, 353; (*e*) P. Braunstein, T. M. Gomes Carneiro, D. Matt, F. Balegroune and D. Grandjean, *Organometallics*, 1989, **8**, 1737; (*f*) P. Berno, P. Braunstein, C. Floriani, A. Chiesi–Villa and C. Guastini, *Inorg. Chem.*, 1991, **30**, 1407; (*g*) P. Braunstein, S. Coco Cea, A. DeCian and J. Fischer, *Inorg. Chem.*, 1992, **31**, 4203; (*h*) P. Braunstein, S. Coco Cea, M. I. Bruce, B. W. Skelton and A. H. White, *J. Chem. Soc.*, *Dalton Trans.*, 1992, 2539; (*i*) P. Braunstein, S. Coco Cea, M. I. Bruce, B. W. Skelton and A. H. White, *J. Organomet. Chem.*, 1992, **423**, C38; (*j*) P. Braunstein, L. Douce, F. Balegroune, D. Grandjean, D. Bayeul, Y. Dusausoy and P. Zanello, *New J. Chem.*, 1992, **16**, 925; (*k*) P. Braunstein, D. J. Kelly, A. Tiripicchio and F. Ugozzoli, *Inorg. Chem.*, 1993, **32**, 4845; (*l*) J. Andrieu, P. Braunstein and A. D. Burrows, *J. Chem. Res.* (*S*), 1993, 380.

2 (*a*) W. Keim, A. Behr, B. Gruber, B. Hoffmann, F. H. Kowaldt, U. Kürschner, B. Limbäcker and F. P. Sistig, *Organometallics*, 1986, **5**, 2356, and references therein; (*b*) W. Keim, *Angew. Chem.*, *Int. Ed. Engl.*, 1990, **29**, 235.

3 See, for example: (*a*) C. J. Moulton and B. L. Shaw, *J. Chem. Soc.*, *Dalton Trans.*, 1980, 299; (*b*) P. Crochet and B. Demerseman, *Organometallics*, 1995, **14**, 2173; (*c*) J. Bank, P. Steinert, B. Windmüller, W. Wolfsberger and H. Werner, *J. Chem. Soc.*, *Dalton Trans.*, 1996, 1153; (*d*) J. Vicente, M.-T. Chicote, M. A. Beswick and M. C. Ramirez de Arellano, *Inorg. Chem.*, 1996, **35**, 6592; (*e*) L. R. Falvello, S. Fernandez, R. Navarro, I. Pascual and E. P. Urriolabeitia, *J. Chem. Soc.*, *Dalton Trans.*, 1997, 763; (*f*) P. Crochet, B. Demerseman, M. I. Vallejo, M. P. Gamasa, J. Gimeno, J. Borge and S. Garcia–Granda, *Organometallics*, 1997, **16**, 5406.

4 P. Braunstein, Y. Chauvin, S. Mercier, L. Saussine, A. DeCian and J. Fischer, *J. Chem. Soc.*, *Chem Commun.*, 1994, 2203.

5 K. A. O. Starzewski and J. Witte, *Angew. Chem.*, *Int. Ed. Engl.*, 1987, **26**, 63.

6 U. Klabunde and S. D. Ittel, *J. Mol. Catal.*, 1987, **41**, 123.

7 K. A. O. Starzewski, in *Ziegler Catalysts*, eds. G. Fink, R. Mülhaupt and H. H. Brintzinger, Springer Verlag, Berlin, 1995.

8 (*a*) P. Braunstein, J. Pietsch, Y. Chauvin, S. Mercier, L. Saussine, A. DeCian and J. Fischer, *J. Chem. Soc.*, *Dalton Trans.*, 1996, 3571; (*b*) J. Andrieu, P. Braunstein and F. Naud, *J. Chem. Soc.*, *Dalton Trans.*, 1996, 2903; (*c*) P. Braunstein, Y. Chauvin, J. Nähring, Y. Dusausoy, D. Bayeul, A. Tiripicchio and F. Uggozoli, *J. Chem. Soc.*, *Dalton Trans.*, 1995, 851; (*d*) P. Braunstein, Y. Chauvin, J. Nähring, A. DeCian and J. Fischer, *J. Chem. Soc.*, *Dalton Trans.*, 1995, 863.

9 P. Braunstein, Y. Chauvin, J. Nähring, A. DeCian, J. Fischer, A. Tiripicchio and F. Uggozoli, *Organometallics*, 1996, **15**, 5551.

10 D. N. Lawson, J. A. Osborn and G. Wilkinson, *J. Chem. Soc. A*, 1966, 1733.

11 A. J. Deeming and B. L. Shaw, *J. Chem. Soc. A*, 1969, 598.

12 G. Deganello, P. Uguagliati, B. Crociani and U. Belluco, *J. Chem. Soc. A*, 1969, 2726.

13 D. Forster, *J. Am. Chem. Soc.*, 1975, **97**, 951.

14 S. Franks, F. R. Hartley and J. R. Chipperfield, *Inorg. Chem.*, 1981, **20**, 3238.

15 (*a*) J. R. Dilworth, J. R. Miller, N. Wheatley, M. J. Baker and J. G. Sunley, *J. Chem. Soc.*, *Chem. Commun.*, 1995, 1579; (*b*) P. M. Maitlis, A. Haynes, G. J. Sunley and M. J. Howard, *J. Chem. Soc.*, *Dalton Trans.*, 1996, 2187; (*c*) J. Rankin, A. C. Benyei, A. D. Poole and D. J. Cole–Hamilton, *J. Chem. Soc.*, *Dalton Trans.*, 1999, 3771; (*d*) L. Gonsalvi, H. Adams, G. J. Sunley, E. Ditzel and A. Haynes, *J. Am. Chem. Soc.*, 1999, **121**, 11233.

16 S. S. Basson, J. G. Leipoldt and J. T. Nel, *Inorg. Chim. Acta*, 1984, **84**, 167.

17 J. A. Venter, J. G. Leipoldt and R. van Eldick, *Inorg. Chem.*, 1991, **30**, 2207.

18 G. J. J. Steyn, A. Roodt and J. G. Leipoldt, *Inorg. Chem.*, 1992, **31**, 3477.

19 M. Cano, J. V. Heras, M. A. Lobo, E. Pinilla and M. A. Monge, *Polyhedron*, 1992, **11**, 2679.

20 (*a*) Y. S. Varshavsky, T. G. Cherkasova, N. A. Buzina and L. S. Bresler, *J. Organomet. Chem.*, 1994, **464**, 239; (*b*) M. R. Galding, T. G. Cherkasova, Y. S. Varshavsky, L. V. Osetrova and A. Roodt, *Rhodium Express*, 1995, 36.

21 Crystal data for **4**: $C_{39}H_{31}O_2P_2RhI_2$, $M = 950.34$, crystal system monoclinic, space group $P2_1/c$, $a = 13.317(2)$, $b = 34.898(6)$, $c = 16.655$ (3) Å, $\beta = 90.22(1)°$, $U = 7740(2)$ Å^3, $Z = 8$, $D_c = 1.747$ g cm^{-3}, $\mu(\text{MoK}_\alpha) = 2.290$ mm^{-1}, $T = 293$ K.

22 M. J. Baker, M. F. Giles, A. G. Orpen, M. J. Taylor and R. J. Watt, *J. Chem. Soc.*, *Chem. Commun.*, 1995, 197.

23 G. Cardaci, G. Reichenbach and G. Bellachioma, *Organometallics*, 1988, **7**, 2475.

24 D. Forster, *Adv. Organomet. Chem.*, 1979, **17**, 255.

25 (*a*) P. J. Davidson, M. F. Lappert and R. Pearce, *Chem. Rev.*, 1976, **76**, 219; (*b*) J. A. Martinho–Simões and J. L. Beauchamp, *Chem. Rev.*, 1990, **90**, 629.

26 (*a*) J. K. Stille and M. T. Regan, *J. Am. Chem. Soc.*, 1973, **96**, 1508; (*b*) M. C. Baird, J. T. Mague, J. A. Osborn and G. Wilkinson, *J. Chem. Soc. A*, 1967, 1347; (*c*) I. C. Douek and G. Wilkinson, *J. Chem. Soc. A*, 1969, 1508; (*d*) D. L. Egglestone, M. C. Baird, C. J. L. Lock and G. Turner, *J. Chem. Soc.*, *Dalton Trans.*,

1977, 1576; (*e*) M. Bassetti, G. J. Sunley and P. M. Maitlis, *J. Chem. Soc., Chem. Commun.*, 1988, 1012; (*f*) M. Bassetti, G. J. Sunley, F. P. Fanizzi and P. M. Maitlis, *J. Chem. Soc., Dalton Trans.*, 1990, 1799.

27 (*a*) A. Wojcicki, *Adv. Organomet. Chem.*, 1973, **11**, 87; (*b*) F. Calderazzo, *Angew. Chem., Int. Ed. Engl.*, 1977, **16**, 299.

28 (*a*) T. C. Flood, J. E. Jensen and J. A. Statler, *J. Am. Chem. Soc.*, 1981, **103**, 4410; (*b*) H. Brunner and H. Vogt, *Angew. Chem., Int. Ed. Engl.*, 1981, **20**, 405; (*c*) H. Brunner and H. Vogt, *Chem. Ber.*, 1981, **114**, 2186; (*d*) H. Brunner, B. Hammer, I. Bernal and M. Draux, *Organometallics*, 1983, **2**, 1595; (*e*) M. Bassetti, L. Mannina and D. Monti, *Organometallics*, 1994, **13**, 3293.

29 J. A. Collman, L. S. Hegedus, J. R. Norton and R. G. Finke, *Principles and Applications of Organotransition Metal Chemistry*, University Science Books, Mill Valley, CA, USA, 1987.

30 S. C. Wright and M. C. Baird, *J. Am. Chem. Soc.*, 1985, **107**, 6899.

31 The synthesis of this compound is reported in the Experimental section and it was only characterized by spectroscopic methods due to purification and crystallization problems.

32 M. J. A. Kraakman, B. de Klerk–Engels, P. P. M. de Lange, K. Vrieze, W. J. J. Smeets and A. L. Spek, *Organometallics*, 1992, **11**, 3774.

33 G. J. Lamprecht, G. J. van Zyl and J. G. Leipoldt, *Inorg. Chim. Acta*, 1989, **164**, 69 and references therein.

34 I. C. Douek and G. Wilkinson, *J. Chem. Soc. A*, 1969, 2604.

35 J. Chatt and B. L. Shaw, *J. Chem. Soc. A*, 1966, 1437.

36 K. Wang, T. J. Emge and A. S. Goldman, *Organometallics*, 1995, **14**, 4929.

37 K. G. van Aswegen, J. G. Leipoldt, I. M. Potgieter, G. J. Lamprecht, A. Roodt and G. J. van Zyl, *Transition Met. Chem.*, 1991, **16**, 369.

38 S. S. Basson, J. G. Leipoldt, I. M. Potgieter, A. Roodt and T. J. van der Walt, *Inorg. Chim. Acta*, 1986, **119**, L9.

39 (*a*) G. M. Sheldrick, SHELXL-93, Universität Göttingen, Göttingen, Germany, 1993; (*b*) G. M. Sheldrick, SHELXS-86, Universität Göttingen, Göttingen, Germany, 1986.

40 OpenMoleN, Interactive Structure Solution, Nonius B.V., Delft, The Netherlands, 1997.